MATERIALS SCIENCE

Exploring a naturally tailored small molecule for stretchable, self-healing, and adhesive supramolecular polymers

Qi Zhang[1], Chen-Yu Shi[1], Da-Hui Qu[1]*, Yi-Tao Long[1], Ben L. Feringa[1,2]*, He Tian[1]*

Polymeric materials with integrated functionalities are required to match their ever-expanding practical applications, but there is always a trade-off between complex material performances and synthetic simplification. A simple and effective synthesis route is reported to transform a small molecule of biological origin, thioctic acid, into a high-performance supramolecular polymeric material, which combines processability, ultrahigh stretchability, rapid self-healing ability, and reusable adhesivity to surfaces. The proposed one-step preparation process of this material involves the mixing of three commercially available feedstocks at mild temperature without any external solvent and a subsequent cooling process that resulted in a dynamic, high-density, and dry supramolecular polymeric network cross-linked by three different types of dynamic chemical bonds, whose cooperative effects in the network enable high performance of this supramolecular polymeric material.

INTRODUCTION

Modern materials require increasingly sophisticated properties and often multiple functions, and meanwhile, ideal materials should be prepared by a facile and low-energy route originated from readily, preferably bio-based, available feedstocks (*1*). For man-made soft polymeric materials (*2*–*8*), diversified properties including moldability (*9*), stretchability (*10*), self-repair (*11*–*14*), adhesivity (*15*, *16*), and recyclability (*17*) have been developed and enabled, even in an integrated fashion (*18*–*25*). These enhanced requirements lead to an increase in the structural complexity and synthetic difficulty, which also increases the cost. Therefore, it is a crucial challenge to prepare polymeric materials with integrated sophisticated properties by extremely simplified routes from bio-based feedstocks. To surmount this problem, development of supramolecular polymers by the self-assembly of functional small molecules is an attractive solution (*26*–*28*). However, elaborate synthesis of precursors is usually required to introduce the desired supramolecular bonds, and in many cases, supramolecular networks typically exhibit fragile mechanical properties. Meanwhile, typical supramolecular polymers usually require additional solvents to support the dynamic properties and strength of the noncovalent interactions, thus resulting in gel networks instead of dry networks.

Thioctic acid (TA) is a naturally existing small molecule and acts as an essential coenzyme for aerobic metabolism in animals. Two types of dynamic chemical bonds, that is, dynamic covalent disulfide bond and noncovalent hydrogen bond (H-bond) of the carboxyl group, exist in this compound. This tailored molecular structure makes TA a potential candidate for the construction of supramolecular polymer networks in a hierarchical self-assembly fashion (Fig. 1A): (i) At 70°C melting temperature of TA, the five-membered ring–containing disulfide bond undergoes thermal-initiated ring-opening polymerization due to dynamic disulfide exchange (*29*, *30*), thus forming the primary linear covalent backbone as a fluidic liquid, and (ii) after cooling, carboxylic side chains dimerized by H-bonds efficiently cross-link the linear poly(TA), hence resulting in a transparent solid polymer. However, the solid polymer exhibits metastable properties. Semicrystalline poly(TA) oligomers reproduce spontaneously after standing for a few minutes because of the inverse ring-closing depolymerization process initiated by the terminal diradicals (*31*).

To overcome the problem of undesired metastability of poly(TA), a divinylic compound, 1,3-diisopropenylbenzene (DIB), was used to quench the terminal diradicals of poly(TA) by inverse vulcanization, thus strengthening the network by covalent cross-linking. Furthermore, iron(III) ions were introduced into the network to act as a strong complex center with carboxylic groups to replace partial weak H-bonds. Therefore, DIB and iron(III) ions together enabled a thermodynamically stable supramolecular poly(TA-DIB-Fe) copolymer network (Fig. 1A). This copolymer was prepared from three commercial feedstocks in an easy, quick, and reproducible route: DIB and ferric chloride ($FeCl_3$) were first dissolved into molten TA liquid at 70°C, and then the resultant solution was slowly cooled down to room temperature (Fig. 1B). Therefore, multigram-scale products can be prepared by this facile method without any special skills, air/water protection, harsh reaction condition, or tedious precursor synthesis. Consequently, a supramolecular polymer network with three different types of dynamic chemical bonds, that is, dynamic covalent disulfide bonds, noncovalent H-bonds, and iron(III)-carboxylate coordinative bonds, was obtained, and the resulting copolymeric material exhibits some excellent properties, such as low-temperature processability, stretchability, autonomous self-healability, adhesivity, and reusability. So far, no other supramolecular polymeric materials with all these features in a single polymeric system have been reported.

RESULTS

Preparation and characterizations

The synthesis route of the poly(TA-DIB-Fe) copolymer involved the one-pot reaction of molten TA liquid, DIB, and $FeCl_3$ (see the "General Information and Materials" section in the Supplementary Materials), resulting in a transparent polymer (Fig. 1C). Unless indicated

[1]Key Laboratory for Advanced Materials and Joint International Research Laboratory of Precision Chemistry and Molecular Engineering, Feringa Nobel Prize Scientist Joint Research Center, School of Chemistry and Molecular Engineering, East China University of Science and Technology, 130 Meilong Road, Shanghai 200237, China. [2]Centre for Systems Chemistry, Stratingh Institute for Chemistry and Zernike Institute for Advanced Materials, Faculty of Mathematics and Natural Sciences, University of Groningen, Nijenborgh 4, 9747 AG Groningen, Netherlands.
*Corresponding author. Email: dahui_qu@ecust.edu.cn (D.-H.Q.); b.l.feringa@rug.nl (B.L.F.); tianhe@ecust.edu.cn (H.T.)

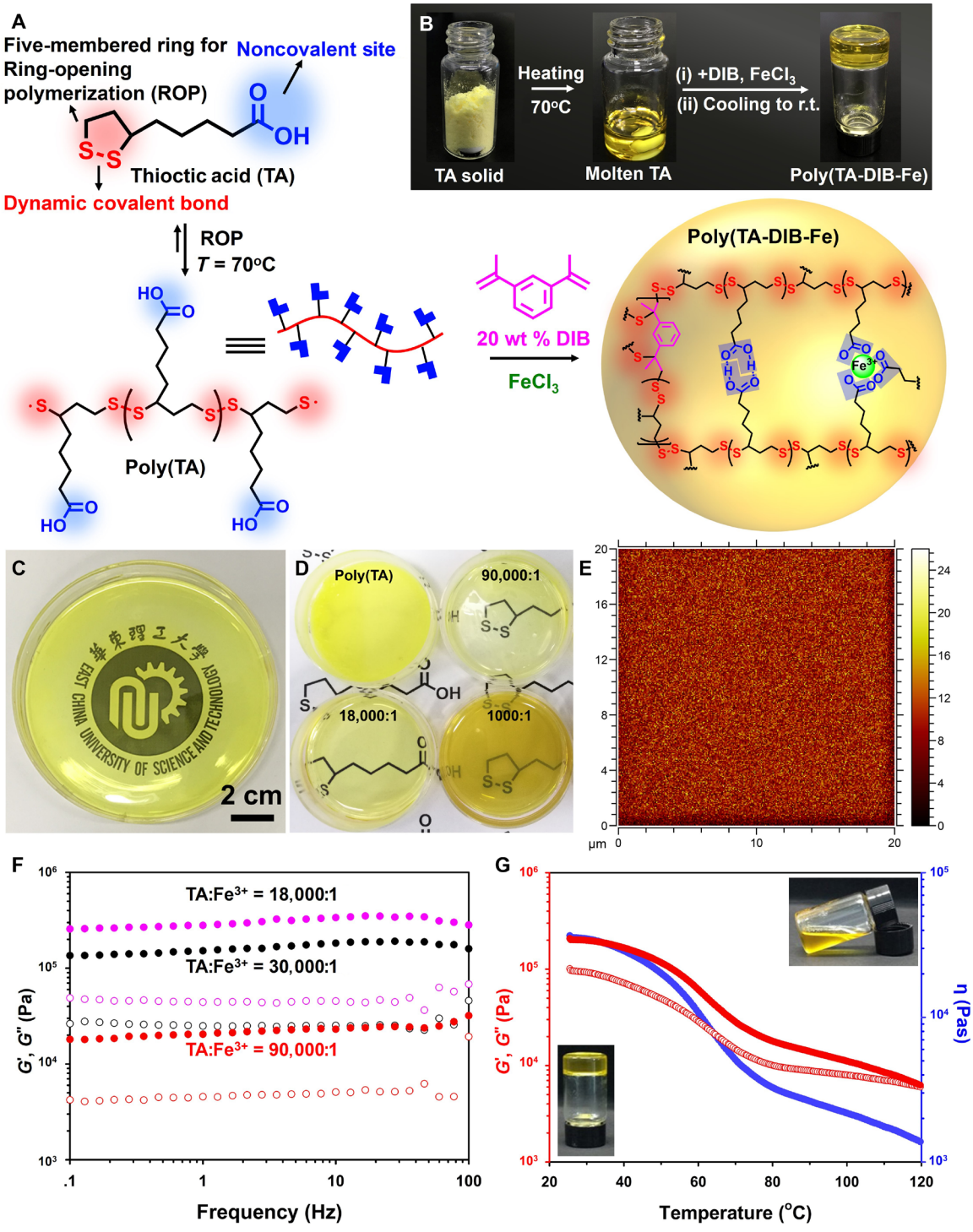

Fig. 1. One-step preparation of the poly(TA-DIB-Fe) copolymer network and its characterization. (**A**) Schematic representation of the synthesis route of the copolymer network. (**B**) Photographs of TA powder, molten TA liquid, and poly(TA-DIB-Fe) copolymer solid. r.t., room temperature. (**C**) The transparent polymeric film prepared by 25-g poly(TA-DIB-Fe) cured in a Petri dish with a TA-to-iron(III) molar ratio of 18,000:1. (**D**) Photographs of poly(TA) and poly(TA-DIB-Fe) film samples synthesized by different TA-to-iron(III) molar ratios. (**E**) Time-of-flight secondary ion mass spectroscopy (TOF-SIMS) mapping images of molecular ion fragments attributed to TA [TA-to-iron(III) molar ratio of 18,000:1]. (**F**) Frequency dependency of storage (solid dots, *G*′) and loss (hollow dots, *G*″) moduli of copolymer network with different iron(III) concentrations. (**G**) Temperature dependency of storage (solid dots, *G*′) and loss (hollow dots, *G*″) moduli and viscosity (blue dots, η) of copolymer network [TA-to-iron(III) molar ratio of 18,000:1]. Inset photographs manifest the transformation from solid to liquid due to the decrease in viscosity by heating.

otherwise, the amount of DIB was set as 20 weight % (wt %) of TA, which enabled the formation of stable, amorphous, and transparent polymer films (fig. S1). The reaction temperature was maintained at 70°C, and the copolymerization reaction was completed in 5 min, thus exhibiting a low energy–consuming preparation method. This facile synthesis process fabricated a robust large-area poly(TA-DIB-Fe) film on a 25-g scale by pouring a molten precursor mixture into a specific mold (Fig. 1C and fig. S2). The resultant poly(TA-DIB-Fe) copolymer films manifested good transparency at different iron(III) concentrations (Fig. 1D), whereas the transparency of the poly(TA) film without the DIB stabilizer was poor because of the coexistence of poly(TA) oligomers.

To reveal its structural characteristics, poly(TA-DIB-Fe) copolymer was characterized by multiple techniques. ^{1}H nuclear magnetic resonance (NMR) spectroscopy confirmed the efficient copolymerization reaction (fig. S3). The Raman peaks (fig. S4) at 501 and 996 cm^{-1} were attributed to the vibration of disulfide bonds and aromatic backbone originated from vulcanized DIB, respectively. The remarkable peak splitting at around 686 cm^{-1} suggested the existence of benzyl-C-S bonds, indicating a successful covalent cross-linking between TA and DIB. The Fourier transform infrared (FTIR) peak at around 3500 cm^{-1} (fig. S5) revealed the presence of H-bonds, and the peak at 1625 cm^{-1} originated from the carbonyl groups of iron(III)-carboxylate coordinative bond. The distribution of the ring-opened TA fragments (Fig. 1E), vulcanized DIB, and iron(III) ions (figs. S6 to S9) in poly(TA-DIB-Fe) copolymer was detected by TOF-SIMS, and the homogeneous species indicated the dry nature of the resulting network owing to the solvent-free preparation method. Scanning electron microscopy (SEM) showed that the surface morphology of the high-density network was free from holes or iron aggregates (figs. S10 and S11). The lability of the copolymer film under a high-energy electron beam (fig. S12) suggested the presence of easily reduced disulfide bonds in the backbone of the resulting polymeric network.

The glass transition temperature (T_g) of poly(TA-DIB-Fe) copolymer was found to be dependent of iron(III) concentrations, and differential scanning calorimetry (DSC) showed that T_g increased from below −20° to 104.8°C with increasing iron(III) concentrations (fig. S13). The absence of the characteristic melting temperature (T_m) at 64.3°C was also evidence for the complete consumption of TA monomers. The amorphous state of the copolymer was further confirmed by the lack of crystalline peaks in x-ray diffraction (XRD) (fig. S14). Notably, no peak of iron oxides was detected in XRD spectra of all the copolymer samples, indicating the absence of iron oxide nanoparticles formed in this copolymer. The initial decomposition temperature of the resulting copolymer was found to be about 200°C by thermogravimetric analysis (TGA) (fig. S15), thus presenting good stability in a broad temperature region. In rheological analysis (Fig. 1F), the storage moduli (G') were higher than the loss moduli (G'') over the entire range of frequencies for all three poly(TA-DIB-Fe) samples, also manifesting a single plateau region in their dynamic moduli. Among the tested samples, the poly(TA-DIB-Fe) copolymer with a TA-to-iron(III) molar ratio of 18,000:1 yielded the highest G' value, thus suggesting superior mechanical strength due to high iron(III) concentration. Moreover, an increase in temperature led to a decrease in viscosity of the copolymer (Fig. 1G) because of the heat-labile H-bonds and dynamic disulfide bonds; consequently, the solid poly(TA-DIB-Fe) copolymer melted into liquid (fig. S16). The strong dependence of viscosities on temperatures allows the materials to be easily processed and molded (fig. S17), and it is one of the typical advantages of supramolecular polymeric materials (*27*).

Mechanical properties

The resulting poly(TA-DIB-Fe) copolymer exhibited excellent mechanical strength; it was pressed without fragmentation and cannot be easily cut by a knife (Fig. 2A). Moreover, the copolymer also exhibited outstanding stretchability (Fig. 2, B and C). A piece of copolymer was stretched into 150 times its original length without breaking (Fig. 2D and fig. S18), and it was partially recovered after release (fig. S19). It is worth noting that such a large rate of breaking elongation is rarely reported in previous studies on supramolecular polymeric materials (*32*). From the low-strain region (<20% strain) of the stress-strain curve in Fig. 2D, the Young's modulus was calculated as 81.4 ± 0.8 kPa, thus indicating the high binding strength of iron(III)-carboxylate coordinative bond. The stress-strain curve involved an initial stiffening region (in which the tension remarkably increased with the increasing strains) followed by a gradual drop in tensile stress with the increasing strains; therefore, it signifies the possible energy dissipation in the network. Moreover, a predamaged network with a notch (the size of the notch was three-fourth of the diameter of the original sample) was also stretched to more than 110 times of its original length without breaking (fig. S20). The creep experiments (fig. S21A) indicated that the resulting network can sustain a load for an extended period. The stress-relaxation experiments (fig. S21B) showed that the instantaneous stress at 100% strain was 36.8 kPa, and subsequently, it was relaxed to 10.4 kPa within 5 min, suggesting fast chain-sliding motion and dynamic bond exchange when stretching the network. The viscous poly(TA-DIB-Fe) copolymer was stretched into filament at 60°C (Fig. 2E and movie S1) by slowly separating two glass slides. The polymeric filament was found to be thinner than hairs (Fig. 2C), thus suggesting an excellent stretchability of the network.

The exceptional stretchability and mechanical strength of the resulting network can be attributed to two key aspects of the proposed mechanism (Fig. 2F): (i) The presence of three different dynamic chemical bonds, such as dynamic covalent disulfide bonds, H-bonds, and iron(III)-carboxylate coordinative bonds, causes the network to stretch by a hierarchical energy dissipation mechanism, and (ii) the dry network bears a large number of high-density cross-linking sites, thus leading to highly folded polymer chains, which allow easier chain sliding due to a decrease in interchain distances. Furthermore, the role of iron(III) ions on the mechanical strength of the poly(TA-DIB-Fe) network was investigated. It was found that the stronger noncovalent cross-linkers [iron(III)-carboxylate coordinative bonds] had profound effects on Young's modulus (Fig. 2G), which increased with the increasing iron(III) concentrations. This mechanism was further corroborated by the decrease in breaking elongations with the increasing strain rates (Fig. 2H). The recovery property of the network was also investigated by the stress-strain curves in different strain regions. In the low-strain region, the stretched network was recoverable (proved by the cycling strain experiments; fig. S22). In the elastic region, the polymeric network was partially recoverable, and in the immediate recovery experiment with multistep strains from 200 to 6400%, it exhibited a reversible elasticity (Fig. 2I).

Self-healing properties

The presence of three types of dynamic chemical bonds also enabled an autonomous self-healing capability in the poly(TA-DIB-Fe)

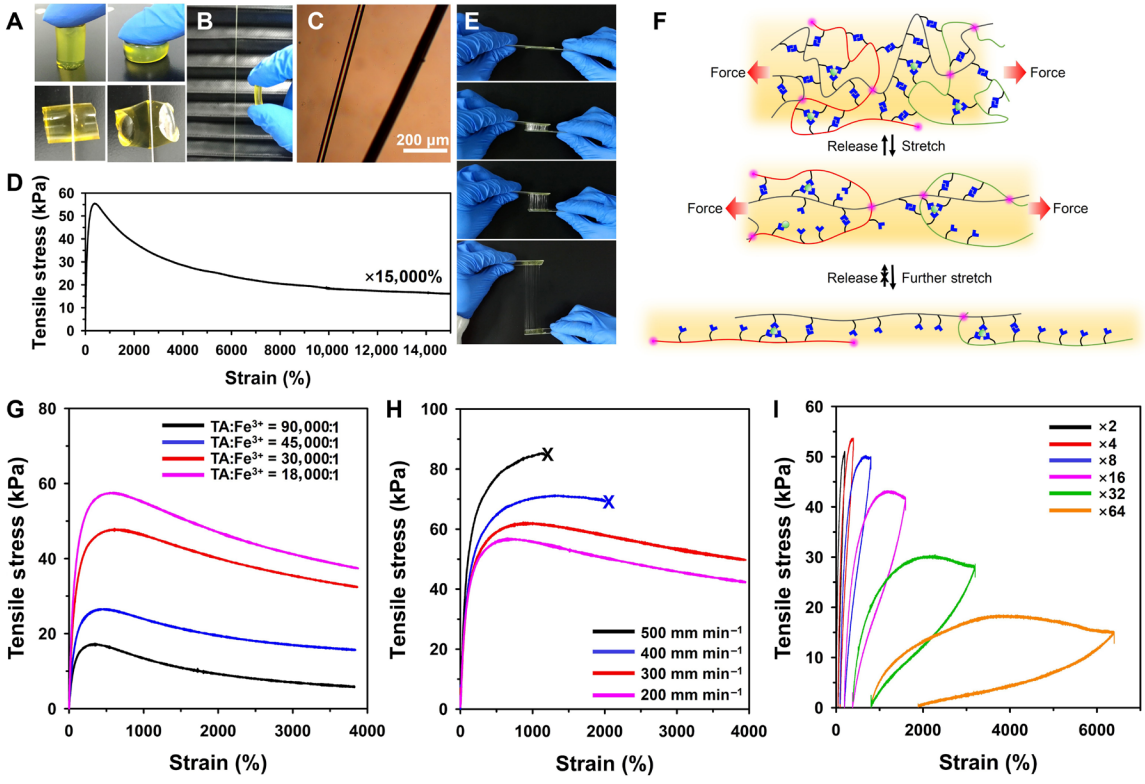

Fig. 2. Mechanical properties of poly(TA-DIB-Fe) copolymer. (**A**) A free-standing copolymer can be pressed without fragmentation and cannot be cut easily with a knife. (**B**) A rod-like copolymer can be stretched into a thin filament. (**C**) Optical microscopy image of a stretched copolymer filament (left) with a human hair (right) as a reference. (**D**) Stress-strain curve of the resulting network [TA-to-iron(III) molar ratio of 18,000:1] for a strain of 15,000%. (**E**) Photographs of the stretchable viscous copolymer adhered between the two glass slices. The copolymer was first preheated to the viscous state and then deposited onto glass surfaces. (**F**) Proposed energy dissipation mechanism for ultrahigh stretchability. (**G**) Stress-strain curves of the copolymer with different iron(III) concentrations. (**H**) Stress-strain curves of the copolymer at varied strain rates [TA-to-iron(III) molar ratio of 18,000:1]. (**I**) Sequential loading-unloading stress-strain curves without rest internals [TA-to-iron(III) molar ratio of 18,000:1]. The successful stretching without breaking proves the resistance of the copolymer to fatigue.

copolymer. It is observable from Fig. 3 (A and B) that a scratch on the resulting copolymer film autonomously healed after 6 hours at room temperature. Moreover, two cut-off rod-shaped copolymers were readily cured by attaching a freshly cut interface, thus resulting in a stretchable healed network (Fig. 3C). Furthermore, the rod-shaped copolymer was constructed into different shapes by mild extrusion and subsequent self-healing (Fig. 3, D to F), thus signifying excellent processability. Moreover, the copolymer also exhibited self-healing capability under water (fig. S23 and movie S2). The copolymer manifested an extremely rapid self-healing behavior at room temperature, and the stress-strain curve of the healed network gained approximately 80% of its original elastic modulus in 1 min and overlapped with the original curve after 5 min of self-healing (Fig. 3G). Such rapid self-healing efficiency without external stimuli is very rare in self-healing materials (*33*, *34*), especially in dry polymeric materials because of their slow chain mobility and the poor dynamics of the dynamic chemical bonds in the absence of solvent (*35*).

Aging inhibits the self-healing capability of supramolecular polymers because of the decreased number of "unbound chemical bonds" or "sticky" bonds, which play a key role in self-healing processes (*11*, *35*). In our experiment, copolymers aged for 24 hours were contacted, slightly extruded, and left for self-healing. The aged copolymers exhibited slower healing rates as compared to the freshly cut ones, and it can be attributed to the lack of sticky bonds. The self-healing process can be completed in 40 hours. The self-healing efficiency of the poly(TA-DIB-Fe) copolymer was measured against healing time at a lower iron(III) concentration [TA-to-iron(III) molar ratio of 90,000:1], and a slower healing rate was detected (Fig. 3H), hence suggesting a significant enhancement of iron(III)-carboxylate coordinative bond during the healing process. The proposed self-healing mechanism is illustrated in Fig. 3I. In fresh samples, the interfacial sticky groups, nonsaturated H-bonds, and iron(III)-carboxylate coordinative bonds formed a new weak interface by noncovalent interactions, and then the disulfur dynamic covalent exchange accelerated the formation of a strong interface by covalent bonding. In aged samples, the noncovalent acceleration process was impeded, and the covalent exchange reaction required an additional breaking and remaking process of disulfide bonds, consequently causing a decrease in the healing rate. Therefore, the resulting poly(TA-DIB-Fe) copolymer can be self-healed in a rapid, water- and aging-resistant manner because of the high-density dynamic chemical bonds.

Application in supramolecular adhesives

Owing to the abundant carboxylic groups in the poly(TA-DIB-Fe) copolymer, the tendency to form hydrogen bonds with polyhydric surfaces makes this copolymer a potential surface adhesive material. The thermoplastic property allowed the polymeric network to transform into a liquid state by heating, and then the liquid copolymer

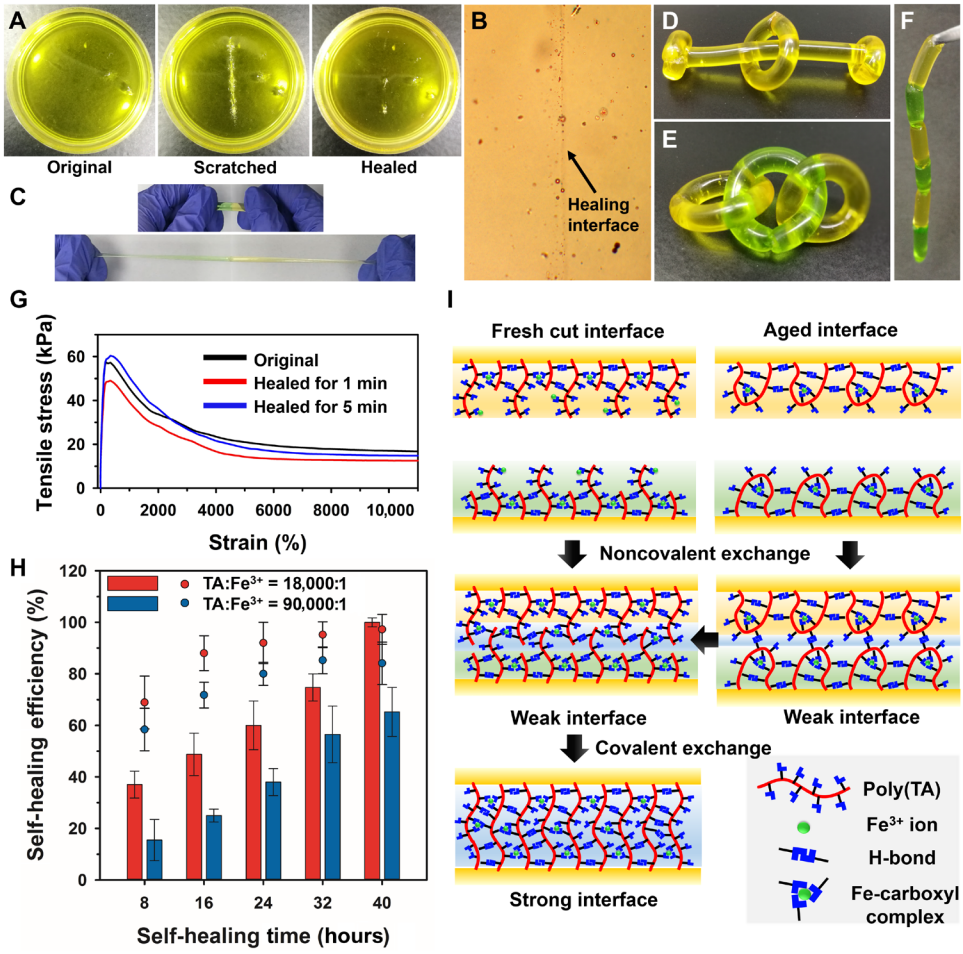

Fig. 3. Self-healing properties of the poly(TA-DIB-Fe) copolymer. (**A**) Photographs depict that a scratch on the copolymer membrane can be autonomously cured after 6 hours at room temperature. (**B**) Optical microscopy image of a healed sample. (**C**) Photographs of a healed film before and after stretching. (**D** to **F**) The rod-shaped copolymer can be used to construct objects of different shapes. (**G**) Stress-strain curves of the healed samples [TA-to-iron(III) molar ratio of 18,000:1] with freshly cut interfaces. (**H**) Dependency of self-healing efficiency of the aged copolymers on time [TA-to-iron(III) molar ratios of 18,000:1 and 90,000:1]. Both the healing efficiencies are presented by the maximal strain (column) and the maximal tensile stress (dot) of the healed samples. (**I**) Proposed self-healing mechanism of the freshly cut and aged interfaces. Error bars show SD with $n = 3$ repeats.

was deposited on a glass slice followed by hot-pressing with another slice of glass (Fig. 4A) to form a transparent film of 50 μm thickness. Subsequent cooling to room temperature enabled the reformation of the poly(TA-DIB-Fe) network between the two glass slices, resulting in high adhesive strength to the adhered glass slices. It is noticeable from Fig. 4B that a weight of 5 kg could be hung up under the two adhered glass slices with a glued area of 2 cm × 2 cm. In the dynamic lifting experiment, the two adhered glass slices were able to lift weights of 27 kg, thus revealing their ultrahigh adhesive strength (movie S3).

Quantitative tests demonstrated the effects of the iron(III)-to-TA molar ratio on adhesive force (Fig. 4B). The shear strength exhibited a linear positive correlation with respect to the iron(III)-to-TA molar ratio, thus indicating the key role of iron(III)-carboxylate coordinative bonds in the enhancement of toughness of poly(TA-DIB-Fe) adhesives. In comparison to commercial glue, the copolymer adhesive material yielded enhanced adhesive forces on nine different tested surfaces (Fig. 4C). Moreover, the resultant copolymer exhibited a remarkable and excellent adhesive capability to hydrophobic Teflon surfaces with a shear strength of 1.00 MPa (*15*). It can be ascribed to the surface spreading and gap-filling capabilities of molten hydrophobic poly(TA-DIB-Fe) liquid for the Teflon surface (*36*) as well as to the adhesive force formed by the high-density H-bonds between the carboxylic groups of the poly(TA-DIB-Fe) copolymer and the hydroxyl groups of hydrophilic surfaces or the fluorine groups of hydrophobic Teflon surface (*37*). The H-bonding adhesive mechanism was verified by the variable temperature experiments on both glass and Teflon surfaces (Fig. 4D and fig. S24), and a decrease in adhesive force was detected with increasing temperatures due to the presence of heat-labile H-bonds. At 60°C, shear strength decreased to 0.01 MPa, and consequently, the adhered surfaces were separated easily. The separated glass slices were again autonomously adhered by the method demonstrated in Fig. 4A. The poly(TA-DIB-Fe) copolymer manifested no fatigue after 30 times cycling experiments (Fig. 4E), hence suggesting its excellent reusability because of the dynamic nature of supramolecular polymeric materials.

DISCUSSION

In this research, a natural monomer small molecule was explored to design supramolecular polymeric materials with integrated functionalities,

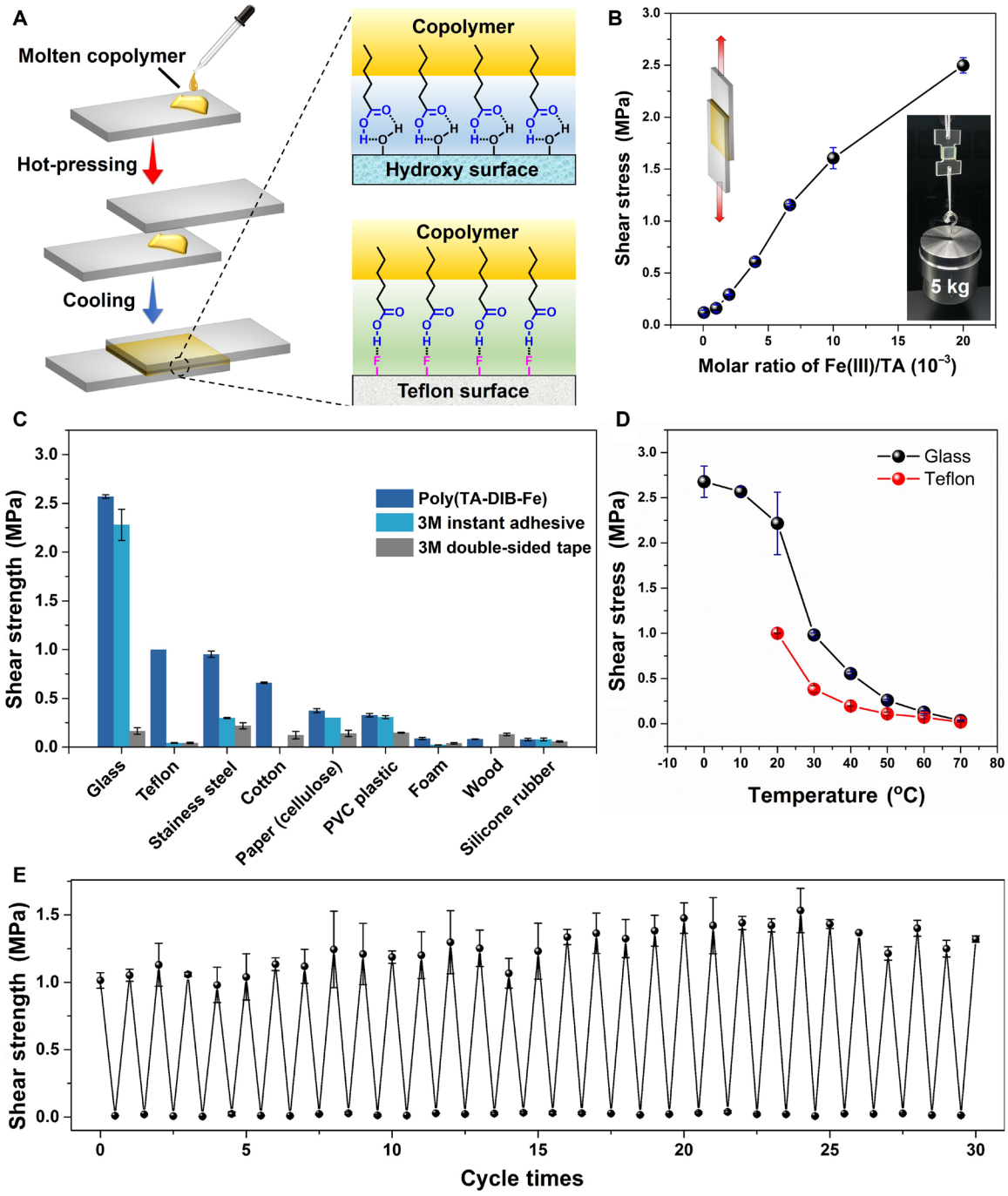

Fig. 4. Application of poly(TA-DIB-Fe) copolymer as adhesive materials. (**A**) Schematic representation of the adhesion procedure. (**B**) Shear strength of the copolymer for different TA-to-iron(III) molar ratios. The inset optical image illustrates the adhesive behavior of the copolymer on glass slices. The adhesion area was 2.0 cm × 2.0 cm, and the weight was 5 kg. (**C**) Comparison of shear strengths between poly(TA-DIB-Fe) copolymer [with a TA-to-iron(III) molar ratio of 50:1] and commercial adhesive materials (3M instant adhesive and double-sided tape) on nine different types of surfaces. PVC, polyvinyl chloride. (**D**) Shear strength versus temperature curves of the copolymer [TA-to-iron(III) molar ratio of 50:1] for the glass and Teflon surfaces. The shear strength for Teflon at below 20°C was too high to be measured because of the limited mechanical strength of the used Teflon film. (**E**) Shear strengths of the copolymer after 30 times cycling experiments [TA-to-iron(III) molar ratio of 150:1]. Error bars present the SDs with $n = 5$ repeats.

such as moldability, stretchability, self-healing capability, and adhesivity. Considering the extremely simplified molecular structure and the facile preparation method, a variety of future supramolecular polymers can be prepared by taking advantages of potential reaction sites of carboxylic groups. Moreover, dry environment and high-density cross-links of the network will amplify the cooperative effects of different dynamic combinations in the polymeric network. Hence, it can be envisioned that this simple copolymer might have major

potentials in the fabrication of adhesives, self-healing materials, and wearable and biodegradable devices.

MATERIALS AND METHODS

Preparation of poly(TA-DIB-Fe) copolymer

TA powder (25 g) was added to a vial and then heated at 70°C in an oil bath. A yellow transparent low-viscosity liquid was obtained after 1 min, and then the stirring was started. DIB (5 g, 20 wt %) was injected under stirring, and the mixture was stirred at 70°C for 5 min. Subsequently, a certain amount of $FeCl_3$ [determined by the molar ratio of TA to iron(III)] was added to the mixture under violent stirring. The liquid mixture was then easily poured into the desired mold, and the yellow transparent solid copolymer was obtained after cooling down to room temperature.

Methods for mechanical test

All stress-strain curves were obtained from an HY-0580 tension machine (HENGYI Company). The cylindrical shaped tested samples (height, 15 mm; diameter, 4.72 mm) were first molded in plastic injection syringes, and the samples were then fixed on the jigs of the tension machine by two glass slices. The initial length (5 mm) was considered as the gap between the two edges of the glass slices. Unless otherwise noted, the tensile stress was measured at a constant speed of 200 mm/min. The data were recorded in real time by a connected computer.

Methods for healing test

The copolymer cylinder (height, 15 mm; diameter, 4.5 mm) was cut into two identical pieces by a knife, and the interfaces were contacted immediately followed by slight extrusion for healing. The stress-strain curves of the healed samples were obtained from the aforesaid mechanical test. The self-healing efficiency was calculated by the ratio of breaking elongation of the healed samples to that of original samples. For the aged samples, the cut interfaces were exposed to air at room temperature for 24 hours and then contacted together for healing.

Methods for adhesive tests

The copolymer solid was melted into low-viscosity liquid by heating, followed by its deposition onto a substrate. The deposition area was fixed as 2.0 cm × 2.0 cm. After the deposition, another substrate was used to hot-press the deposited copolymer liquid. The thickness of the copolymer between the two substrates was 50 μm, which was precisely controlled by quartz powder added between the substrates. The cooling process was controlled by a hot plate at a rate of 5°C/min. The shear strength experiments were performed on an HY-0580 tension machine (HENGYI Company). The two substrates adhered between the two fixtures in a vertical direction. The strain rate was 5 mm/min, and the data were recorded in real time.

SUPPLEMENTARY MATERIALS

Supplementary material for this article is available at http://advances.sciencemag.org/cgi/content/full/4/7/eaat8192/DC1

General Information and Materials

Fig. S1. Photograph of the poly(TA) and poly(TA-DIB) samples with different amounts of DIB.

Fig. S2. Photograph of the molten TA of a 25-g scale mixed with DIB and $FeCl_3$.

Fig. S3. NMR analysis.

Fig. S4. Raman spectrum of the poly(TA-DIB-Fe) copolymer.

Fig. S5. FTIR characterization.

Fig. S6. TOF-SIMS of the cation fragments of the poly(TA-DIB-Fe) copolymer.

Fig. S7. TOF-SIMS mapping images of the cation fragments of the poly(TA-DIB-Fe) copolymer.

Fig. S8. TOF-SIMS of the anion fragments of the poly(TA-DIB-Fe) copolymer.

Fig. S9. TOF-SIMS mapping images of the anion fragments of the poly(TA-DIB-Fe) copolymer.

Fig. S10. SEM images of the poly(TA-DIB-Fe) copolymer.

Fig. S11. Energy-dispersive spectroscopy spectrum and elementary mapping images of the poly(TA-DIB-Fe) copolymer.

Fig. S12. SEM image of the electron-reduced copolymer film.

Fig. S13. DSC analysis.

Fig. S14. XRD analysis.

Fig. S15. TGA of the poly(TA-DIB-Fe) copolymer.

Fig. S16. Photographs of the reversible solid-liquid transition of the poly(TA-DIB-Fe) copolymer.

Fig. S17. Photographs showing the thermal remolding of the poly(TA-DIB-Fe) copolymer.

Fig. S18. Photograph of the poly(TA-DIB-Fe) copolymer after being stretched to 15,000% of its original length.

Fig. S19. Photograph of the partially recovered copolymer.

Fig. S20. Tensile experiment with predamaged copolymer.

Fig. S21. Creep and stress-relaxation experiments of the copolymer.

Fig. S22. Cyclic stress-strain tests.

Fig. S23. Photographs of the self-healing experiment under water.

Fig. S24. Loading curves for poly(TA-DIB-Fe) copolymer adhesives.

Movie S1. The viscous poly(TA-DIB-Fe) copolymer between the two slides of glass at a temperature of 60°C can be stretched into filaments by slowly separating the two slides of glass.

Movie S2. The video shows the self-healing capability of the copolymer under water.

Movie S3. In a dynamic lifting experiment, the two adhered glass slices can also be used to lift weights of 27 kg.

REFERENCES AND NOTES

1. J.-F. Lutz, J.-M. Lehn, E. W. Meijer, K. Matyjaszewski, From precision polymers to complex materials and systems. *Nat. Rev. Mater.* **1**, 16024 (2016).
2. T. Aida, E. W. Meijer, S. I. Stupp, Functional supramolecular polymers. *Science* **335**, 813–817 (2012).
3. R. J. Wojtecki, M. A. Meador, S. J. Rowan, Using the dynamic bond to access macroscopically responsive structurally dynamic polymers. *Nat. Mater.* **10**, 14–27 (2011).
4. D. B. Amabilino, D. K. Smith, J. W. Steed, Supramolecular materials. *Chem. Soc. Rev.* **46**, 2404–2420 (2017).
5. L. Yang, X. Tan, Z. Wang, X. Zhang, Supramolecular polymers: Historical development, preparation, characterization, and functions. *Chem. Rev.* **115**, 7196–7239 (2015).
6. J. H. van Esch, B. L. Feringa, New functional materials based on self-assembling organogels: From serendipity towards design. *Angew. Chem. Int. Ed.* **39**, 2263–2266 (2000).
7. C. J. Hawker, K. L. Wooley, The convergence of synthetic organic and polymer chemistries. *Science* **309**, 1200–1205 (2005).
8. X. Ma, H. Tian, Stimuli-responsive supramolecular polymers in aqueous solution. *Acc. Chem. Res.* **47**, 1971–1981 (2014).
9. B. J. B. Folmer, R. P. Sijbesma, R. M. Versteegen, J. A. J. van der Rijt, E. W. Meijer, Supramolecular polymer materials: Chain extension of telechelic polymers using a reactive hydrogen-bonding synthon. *Adv. Mater.* **12**, 874–878 (2000).
10. T. Sekitani, Y. Noguchi, K. Hata, T. Fukushima, T. Aida, T. Someya, A rubberlike stretchable active matrix using elastic conductors. *Science* **321**, 1468–1472 (2008).
11. P. Cordier, F. Tournilhac, C. Soulié-Ziakovic, L. Leibler, Self-healing and thermoreversible rubber from supramolecular assembly. *Nature* **451**, 977–980 (2008).
12. B. Ghosh, M. W. Urban, Self-repairing oxetane-substituted chitosan polyurethane networks. *Science* **323**, 1458–1460 (2009).
13. M. Burnworth, L. Tang, J. R. Kumpfer, A. J. Duncan, F. L. Beyer, G. L. Fiore, S. J. Rowan, C. Weder, Optically healable supramolecular polymers. *Nature* **472**, 334–337 (2011).
14. Y. Yanagisawa, Y. Nan, K. Okuro, T. Aida, Mechanically robust, readily repairable polymers via tailored noncovalent cross-linking. *Science* **359**, 72–76 (2018).
15. C. Heinzmann, C. Weder, L. M. de Espinosa, Supramolecular polymer adhesives: Advanced materials inspired by nature. *Chem. Soc. Rev.* **45**, 342–358 (2016).
16. S. Lamping, T. Otremba, B. J. Ravoo, Carbohydrate-responsive surface adhesion based on the dynamic covalent chemistry of phenylboronic acid- and catechol-containing polymer brushes. *Angew. Chem. Int. Ed.* **57**, 2474–2478 (2018).
17. Y. Nishimura, J. Chung, H. Muradyan, Z. Guan, Silyl ether as a robust and thermally stable dynamic covalent motif for malleable polymer design. *J. Am. Chem. Soc.* **139**, 14881–14884 (2017).
18. Q. Wang, J. L. Mynar, M. Yoshida, E. Lee, M. Lee, K. Okuro, K. Kinbara, T. Aida, High-water-content mouldable hydrogels by mixing clay and a dendritic molecular binder. *Nature* **463**, 339–343 (2010).
19. J. Y. Oh, S. Rondeau-Gagné, Y.-C. Chiu, A. Chortos, F. Lissel, G.-J. N. Wang, B. C. Schroeder, T. Kurosawa, J. Lopez, T. Katsumata, J. Xu, C. Zhu, X. Gu, W.-G. Bae, Y. Kim, L. Jin,

J. W. Chung, J. B.-H. Tok, Z. Bao, Intrinsically stretchable and healable semiconducting polymer for organic transistors. *Nature* **539**, 411–415 (2016).
20. C.-H. Li, C. Wang, C. Keplinger, J.-L. Zuo, L. Jin, Y. Sun, P. Zheng, Y. Cao, F. Lissel, C. Linder, X.-Z. You, Z. Bao, A highly stretchable autonomous self-healing elastomer. *Nat. Chem.* **8**, 618–624 (2016).
21. G. A. Williams, R. Ishige, O. R. Cromwell, J. Chung, A. Takahara, Z. Guan, Mechanically robust and self-healable superlattice nanocomposites by self-assembly of single-component "sticky" polymer-grafted nanoparticles. *Adv. Mater.* **27**, 3934–3941 (2015).
22. J. Cui, D. Daniel, A. Grinthal, K. Lin, J. Aizenberg, Dynamic polymer systems with self-regulated secretion for the control of surface properties and material healing. *Nat. Mater.* **14**, 790–795 (2015).
23. E. Filippidi, T. R. Cristiani, C. D. Eisenbach, J. H. Waite, J. N. Israelachvili, B. K. Ahn, M. T. Valentine, Toughening elastomers using mussel-inspired iron-catechol complexes. *Science* **358**, 502–505 (2017).
24. H. Chen, X. Ma, S. Wu, H. Tian, A rapidly self-healing supramolecular polymer hydrogel with photostimulated room-temperature phosphorescence responsiveness. *Angew. Chem. Int. Ed.* **53**, 14149–14152 (2014).
25. J. Kang, D. Son, G.-J. N. Wang, Y. Liu, J. Lopez, Y. Kim, J. Y. Oh, T. Katsumata, J. Mun, Y. Lee, L. Jin, J. B.-H. Tok, Z. Bao, Tough and water-insensitive self-healing elastomer for robust electronic skin. *Adv. Mater.* **30**, e1706846 (2018).
26. J.-M. Lehn, Supramolecular chemistry—Scope and perspectives molecules, supermolecules, and molecular devices (Nobel Lecture). *Angew. Chem. Int. Ed.* **27**, 89–112 (1988).
27. L. Brunsveld, B. J. B. Folmer, E. W. Meijer, R. P. Sijbesma, Supramolecular polymers. *Chem. Rev.* **101**, 4071–4098 (2001).
28. T. F. A. de Greef, E. W. Meijer, Materials science: Supramolecular polymers. *Nature* **453**, 171–173 (2008).
29. K. Endo, T. Yamanaka, Copolymerization of lipoic acid with 1,2-dithiane and characterization of the copolymer as an interlocked cyclic polymer. *Macromolecules* **39**, 4038–4043 (2006).
30. X. Zhang, R. M. Waymouth, 1,2-dithiolane-derived dynamic, covalent materials: Cooperative self-assembly and reversible cross-linking. *J. Am. Chem. Soc.* **139**, 3822–3833 (2017).
31. W. J. Chung, J. J. Griebel, E. T. Kim, H. Yoon, A. G. Simmonds, H. J. Ji, P. T. Dirlam, R. S. Glass, J. J. Wie, N. A. Nguyen, B. W. Guralnick, J. Park, Á. Somogyi, P. Theato, M. E. Mackay, Y.-E. Sung, K. Char, J. Pyun, The use of elemental sulfur as an alternative feedstock for polymeric materials. *Nat. Chem.* **5**, 518–524 (2013).
32. X. Yan, Z. Liu, Q. Zhang, J. Lopez, H. Wang, H.-C. Wu, S. Niu, H. Yan, S. Wang, T. Lei, J. Li, D. Qi, P. Huang, J. Huang, Y. Zhang, Y. Wang, G. Li, J. B.-H. Tok, X. Chen, Z. Bao, Quadruple H-bonding crosslinked supramolecular polymeric materials as substrates for stretchable, antitearing, and self-healable thin film electrodes. *J. Am. Chem. Soc.* **140**, 5280–5289 (2018).
33. H. Qin, T. Zhang, H.-N. Li, H.-P. Cong, M. Antonietti, S.-H. Yu, Dynamic Au-thiolate interaction induced rapid self-healing nanocomposite hydrogels with remarkable mechanical behaviors. *Chem. Rev.* **3**, 691–705 (2017).
34. R. P. Wool, Self-healing materials: A review. *Soft Matter* **4**, 400–418 (2008).
35. N. Roy, B. Bruchmann, J.-M. Lehn, DYNAMERS: Dynamic polymers as self-healing materials. *Chem. Soc. Rev.* **44**, 3786–3807 (2015).
36. A. H. Hofman, I. A. van Hees, J. Yuan, M. Kamperman, Bioinspired underwater adhesives by using the supramolecular toolbox. *Adv. Mater.* **30**, 1704640 (2018).
37. B. Coupe, M. E. Evangelista, R. M. Yeung, W. Chen, Surface modification of poly(tetrafluoroethylene-co-hexafluoropropylene) by adsorption of functional polymers. *Langmuir* **17**, 1956–1960 (2001).

Acknowledgments: We thank the Research Center of Analysis and Test of East China University of Science and Technology for help on the material characterization. We also appreciate X. Hua, Y.-M. Wang, H.-W. Li, and Y.-S. Xu (East China University of Science and Technology) for their help. **Funding:** We thank the support of the National Natural Science Foundation of China (grants 21790361, 21421004, 21672060, and 21788102), the Fundamental Research Funds for the Central Universities (grants WJ1616011, WJ1213007, and 222201717003), the Programme of Introducing Talents of Discipline to Universities (grant B16017), and the Shanghai Science and Technology Committee (grant 17520750100). **Author contributions:** Q.Z., D.-H.Q., B.L.F., and H.T. conceived, designed, and directed the project. Q.Z. and C.-Y.S. performed the experiments. Y.-T.L. supported and performed the TOF-SIMS characterization. Q.Z., D.-H.Q., B.L.F., and H.T. wrote the paper. All authors analyzed the data, discussed the results, and commented on the manuscript. **Competing interests:** D.-H.Q., C.-Y.S., Q.Z., and H.T. are inventors on a provisional patent application related to this work that has been filed by the East China University of Science and Technology (serial no. 2018032100796160, date: 21 March 2018). The authors declare no other competing interests. **Data and materials availability:** All data needed to evaluate the conclusions in the paper are present in the paper and/or the Supplementary Materials. Additional data related to this paper may be requested from the authors.

Submitted 8 April 2018
Accepted 18 June 2018
Published 27 July 2018
10.1126/sciadv.aat8192

Citation: Q. Zhang, C.-Y. Shi, D.-H. Qu, Y.-T. Long, B. L. Feringa, H. Tian, Exploring a naturally tailored small molecule for stretchable, self-healing, and adhesive supramolecular polymers. *Sci. Adv.* **4**, eaat8192 (2018).